Available online at www.sciencedirect.com
SCIENCE DIRECT®
Brain Research 1004 (2004) 1–7
BRAIN RESEARCH
www.elsevier.com/locate/brainres

Research report

# Spinal interneurons infected by renal injection of pseudorabies virus in the rat

Xiaorui Tang, Nathan D. Neckel, Lawrence P. Schramm*

*Departments of Biomedical Engineering and Neuroscience, The Johns Hopkins University School of Medicine, 606 Traylor Building, 720 Rutland Avenue, Baltimore, MA 21205, USA*

Accepted 5 January 2004

**Abstract**

The potency of spinal sympathetic reflexes is increased after spinal injury, and these reflexes may result in life-threatening hypertensive crises in humans. Few, if any, primary afferents project directly to sympathetic preganglionic neurons (SPN). Therefore, spinal sympathetic interneurons (IN) must play a major role in generating dysfunctional sympathetic activity after spinal cord injury. Furthermore, these IN are potentially aberrant targets, either for ascending and descending axons that may sprout after spinal cord injury or for axons that regenerate after spinal cord injury. We identified IN via the transsynaptic retrograde transport of pseudorabies virus (PRV) injected into the kidneys of rats. The proportion of infected IN ranged from approximately 1/3 to approximately 2/3 of the number of infected SPN. IN were heavily concentrated among the SPN in spinal lamina VII. However, IN were located in all lamina of the dorsal horn. The longitudinal distribution of infected IN was closely correlated with the longitudinal distribution of infected SPN. Few infected IN were found rostral or caudal to the longitudinal range of infected SPN. Infected IN were heterogeneous in both their sizes and the extent of their dendritic trees. The strong correlation between longitudinal distributions of infected IN and SPN supports physiological data demonstrating a segmental organization of spinal sympathetic reflexes. The paucity of infected IN in segments distant from SPN suggests that multisegmental sympathetic reflexes are mediated by projections onto IN rather than onto SPN themselves. The morphological heterogeneity of IN probably manifests the variety of systems that affect spinal sympathetic regulation.


*Theme:* Endocrine and autonomic regulation
*Topic:* Cardiovascular regulation

*Keywords:* Spinal sympathetic interneuron; Sympathetic preganglionic neuron; Central cardiovascular regulation; Pseudorabies virus; Spinal cord injury

## 1. Introduction

Brainstem projections to sympathetic preganglionic neurons (SPN) have received substantial attention because levels of ongoing and reflex-elicited sympathetic activity are largely regulated by those synaptic antecedents in spinally intact mammals (see Refs. [3,20] for review). A further motivation for emphasizing brainstem inputs to SPN is the observation that, although primary afferents project into the region of the intermediolateral column of thoracic spinal cord (see, for instance, Ref. [19]), there is little evidence for synapses of these afferents directly onto SPN.

However, SPN do receive input from spinal sympathetic interneurons (IN). These IN have been identified anatomically by transsynaptic infection with pseudorabies virus (PRV) or herpes simplex virus injected into the kidney [21,29] or spleen [6], by their transsynaptic uptake of the beta fragment of cholera toxin injected into the superior cervical ganglion [4], by their infection with herpes simplex injected into the adrenal gland [15,21,36], and by the location of their somas and the morphology and trajectories of their axons [12]. Physiological evidence suggests that spinal IN play a role in spinal sympathetic processing [2,7,8,27]. However, several laboratories, including ours, have shown that spinal sympathetic reflexes are usually tonically inhibited, probably by brainstem systems [9,11,16,28].

Although the role of spinal sympathetic reflexes in normal autonomic regulation may be uncertain, at least

* Corresponding author. Tel.: +1-410-955-3026; fax: +1-410-955-9826.
*E-mail address:* LSCHRAMM@BME.JHU.EDU (L.P. Schramm).

0006-8993/$ - see front matter © 2004 Elsevier B.V. All rights reserved.
doi:10.1016/j.brainres.2004.01.016

three motivations exist for studying spinal sympathetic circuitry. Firstly, experimental spinal cord transection exposes or accentuates spinal sympathetic reflexes [9,11,17,25], and, in humans with spinal cord injury, these reflexes may cause severe, life-threatening hypertensive crises [22,35]. Secondly, although monosynaptic projections of brainstem autonomic systems onto SPN are well documented [24,26], almost nothing is known about projections of these same systems onto spinal sympathetic IN. Thirdly, regenerating or sprouting [38] spinal cord pathways after spinal cord injury in humans may make inappropriate synapses on spinal sympathetic IN, leading to autonomic dysfunction.

Recently, we identified a population of spinal neurons whose ongoing and reflex-evoked activities were closely correlated with ongoing renal sympathetic nerve activity (RSNA), and we hypothesized that they were IN that belong to spinal systems capable of increasing or decreasing RSNA [7,8,18,23]. Significantly, the receptive fields from which both noxious and innocuous stimuli excited these neurons were enlarged after chronic spinal injury [18]. We have precisely located and morphologically characterized a small population of these sympathetically correlated neurons using extracellular recording followed by juxtacellular labeling [34]. Although juxtacellular labeling of sympathetically correlated spinal neurons resulted in both excellent physiological and anatomical characterization, this method was arduous for the identification of large numbers of neurons. Furthermore, the yield of juxtacellularly labeled neurons too very small to combine with simultaneous anterograde tracing of brainstem or spinal pathways in future experiments.

Therefore, in the present study, we identified, localized, and anatomically characterized sympathetic IN by the retrograde, transsynaptic transport of PRV from the kidney. PRV injected into the kidney is transported retrogradely within the axons of sympathetic postganglionic neurons and infects those neurons [13,29,31,32]. Virus produced in sympathetic postganglionic neurons passes transsynaptically to the axons of SPN, which are infected in turn. Virus produced in SPN subsequently infects synaptic antecedents to those SPN, among them spinal sympathetic interneurons. Therefore, only IN that project to SPN that, in turn, potentially play a role in regulating the renal circulation or renal function become infected. This method identified hundreds of IN in each rat. This was a large enough sample to determine the cross-sectional and longitudinal distributions and the somatic and proximal dendritic morphology of these IN.

## 2. Materials and methods

All procedures used in these experiments were approved by the Johns Hopkins University Committee on Animal Care and Use. Thirty-four male, Sprague–Dawley rats (Charles River), weighing between 275 and 350 g were used in these experiments. As reported previously [29], renal injection of PRV resulted in a range of severity of infection. Our criteria for an acceptable severity of infection were (1) that rats exhibit infection of both SPN and IN, and (2) that rats exhibit no infected α-motoneurons. We excluded rats with infected α-motoneurons because the route of infection of those neurons after injection of viruses into abdominal organs is controversial [5], and IN infected via synapses on α-motoneurons might be involved solely in somatic, rather than sympathetic, spinal systems. Three rats were excluded because they exhibited infection of SPN but not IN. Twenty-seven rats were excluded because they exhibited infected α-motoneurons. Therefore, of the thirty-four rats infected for this study, we report results from the four rats that met our criteria.

An amount of 1 to 3 mg of hydroxystilbamidine (HSB, Molecular Probes, Eugene, OR) was delivered to each rat ip. HSB is the active ingredient in Fluorogold® [37]. This procedure quantitatively labels all SPN [1]. Five to ten days after injection with HSB, rats were anesthetized with halothane (5% induction, 2–3% maintenance). The left kidney was approached through a left flank laparotomy and injected with 1 μl of $10^8$ PFU Bartha strain PRV (kindly provided by Dr. Arthur Loewy, Washington University, St. Louis, MO.) in each of two injection sites using a 26 ga Hamilton syringe (Hamilton, Reno, NV). Injections were uniformly placed at sites on the longitudinal midline of the convex surface of the kidney. Injection sites were located by dividing this midline in thirds and injecting at the rostral and caudal end of the middle third. Care was taken to prevent exposure of surrounding tissue to PRV. Injection sites were sealed with a drop of cyanoacrylate, and the incision was closed in two layers. Before cessation of anesthesia, rats were treated with an analgesic, Benamine (1.1 mg/kg, sc) and an antibiotic, Penlog-s (20,000 units, im). Rats were observed carefully several times each day to ensure that they showed no signs of discomfort. Rats ate, drank, and gained weight during this postinfection survival period.

Seventy-two hours after infection, rats were reanesthetized with halothane, injected with 1 g of urethane dissolved in water to sustain anesthesia during perfusion, and perfused transcardially with 300 ml of phosphate buffered saline (PBS) followed by 300 ml of 4% paraformaldehyde in PBS. Spinal cords and brains were removed and postfixed in 4% paraformaldehyde overnight and placed in 30% sucrose in PBS until they no longer floated. The right sides of spinal cords were marked with dorsoventral pinholes at the midpoints of the dorsal root entry zones of spinal segments $T_2$, $T_6$, $T_{10}$, and $L_1$ and cut into four blocks. The rostral and caudal ends of these blocks were the midpoints of the dorsal root entry zones of spinal segments $C_8$–$T_4$, $T_4$–$T_8$, $T_8$–$T_{12}$, and $T_{12}$–$L_3$, respectively. Serial sections of spinal cord were cut horizontally at a thickness of 40 μ beginning at the surface of the dorsal columns and ending at the disappearance of the ventral horn.

Preliminary experiments indicated that the most likely locus of infected α-motoneurons was between $T_8$ and $T_{12}$. These preliminary experiments also indicated that rats exhibiting infected IN at any level also exhibited infected IN between $T_8$ and $T_{12}$. Therefore, we first cut sections of the $T_8$–$T_{12}$ block of spinal cord and processed them, as described below, for visualization of PRV. These sections were inspected to determine whether rats met our criteria, infection of IN but no infection of α-motoneurons. Then, the remaining blocks from rats that met those criteria were similarly cut and processed. The resulting serial sections were inspected, and any rats that exhibited infected α-motoneurons in the additional sections were excluded.

Sections were rinsed three times in PBS and incubated overnight at 4 °C in a solution containing an antibody to PRV made in pig (1:10,000, kindly provided by Dr. Arthur Loewy). Then, sections were rinsed three times in PBS and incubated in goat antipig–Cy3 (1:200, Jackson Immuno Laboratories, West Grove, PA). Labeled sections were washed three times in PBS, mounted serially on slides, and coverslipped. Sections were examined and photographed using green excitation for Cy3 and ultraviolet excitation for HSB.

Histological analysis was conducted in two steps. Firstly, we located all SPN and IN rostrocaudally and mediolaterally with respect to several landmarks (described below), and dorsoventrally with respect to their distances from the central canal. Secondly, using an in-house, geometrical transformation program, we generated composite reconstructions of the locations of neurons on representative horizontal and transverse planes (as shown in the middle and lower panels of Fig. 2, A–D). These procedures are described in more detail below.

We examined all serial sections from all blocks containing spinal segments $C_8$ to $L_3$. Sections were photographed with either 4× or 10× objectives and a dark-field condenser. This method delineated the gray matter–white matter borders and the topography of the spinal laminae. In each section, we located all infected SPN and IN at a resolution of 40 μ rostrocaudally, using as reference points the rostral and caudal ends of each block, and the pin hole indicating that block's middle segment (see above). We measured the mediolateral position of each neuron at the same resolution using the lateral border of the gray matter and the midline as references. The dorsoventral position of each neuron was estimated by counting the number of 40 μ sections between the section containing the neuron and the section containing the center of the central canal at the neuron's rostrocaudal position. The positions of all neurons were marked on photographs of their respective sections. The positions of neurons were geometrically transformed into transverse projections. The resulting projections were then slightly scaled both dorsoventrally and mediolaterally to register them with a standardized transverse thoracic section. Finally, the transformed positions of selected neurons that lay at laminar borders were checked against the photographs of those neurons to ensure that registration was correct. Photographs were taken and distances were measured using *Spot*® software (Diagnostic Instruments, Sterling Heights, MI).

Because the nuclei of infected neurons were usually obscured by PRV labeling, we were sometimes unable to distinguish complete from incomplete neurons. Therefore, we did not attempt to correct for double counting of neurons that had portions of their somas in different sections. For this reason, some SPN and IN may have been counted twice. On the other hand, we did not count profiles with minor axes smaller than 10 μ unless they exhibited substantial dendritic trees. Therefore, some small IN may not have been counted.

## 3. Results

Interneurons were identified as neurons that were infected by PRV but were not labeled with HSB (see Fig. 1 and

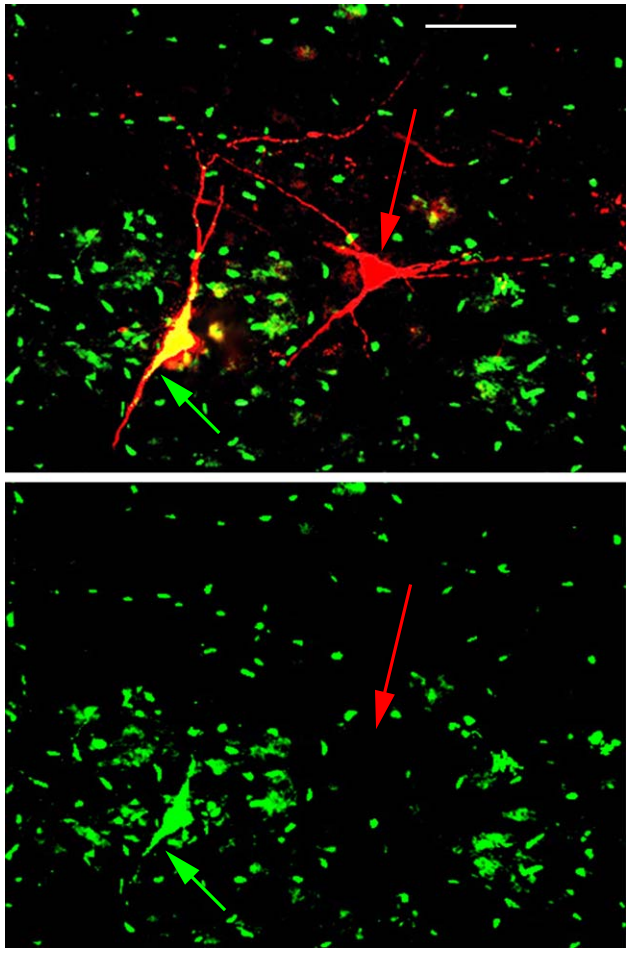

Fig. 1. Identification of interneurons. Top panel: green excitation of infected sympathetic preganglionic neuron (green arrow) and infected IN (red arrow). Bottom panel: UV excitation of same field. The sympathetic preganglionic neuron (green) is still visible by virtue of its labeling with HSB. The infected IN is no longer visible. Scale=40 μ.

Materials and methods). In the four rats reported herein, we observed 252, 205, 356, and 217 infected IN and 366, 625, 518, and 473 infected SPN. Therefore, the ratio of infected IN to infected SPN was 0.68, 0.33, 0.68, and 0.46, respectively.

As reported previously [29], the proportion of the total number of SPN infected by PRV varied greatly along the longitudinal course of each spinal cord. At the longitudinal position in each spinal cord where the largest numbers of SPN were infected, this proportion was approximately 80% of the total number of SPN.

Longitudinally, regions containing larger numbers of infected SPN also contained larger numbers of infected IN (Fig. 2, upper panels). Infected SPN extended approximately one spinal segment more rostrally than infected IN. The distributions of infected IN and SPN ended at similar levels caudally (Fig. 2A–D, upper panels). In three rats (Fig. 2A,B and C) the greatest number of infected neurons was located between $T_{11}$ and $T_{13}$. The longitudinal distribution of infected neurons in these three rats was not symmetrical; the number of infected neurons decreased more rapidly caudally than rostrally. The fourth rat (Fig. 2D) exhibited a more uniform longitudinal distribution of infected neurons. The mediolateral distribution of infected neurons varied with thoracic level (Fig. 2, middle panels). Rostrally, both infected SPN and infected IN were located almost exclusively in the intermediolateral column or in the lateral funiculus. Caudally, infected neurons were distributed more evenly across the intermediate zone.

Analysis of infected SPN and IN in transverse projections (Fig. 2, lower panels) indicated that infected SPN were located almost exclusively from deep in the left dorsolateral funiculus (ipsilateral to the injected kidney) to lamina X. Although several infected IN were located in the most medial portion of lamina X, neither infected IN nor infected SPN were observed on the right (contralateral) side of the spinal cord. In all rats, we identified infected IN in spinal laminae II, III, IV, V, VII, and X. However, this distribution varied both between rats and within rats, at different rostrocaudal levels (Fig. 2, middle and lower panels). In all rats, infected IN were most abundant interspersed among the SPN of the intermediolateral column. Their number

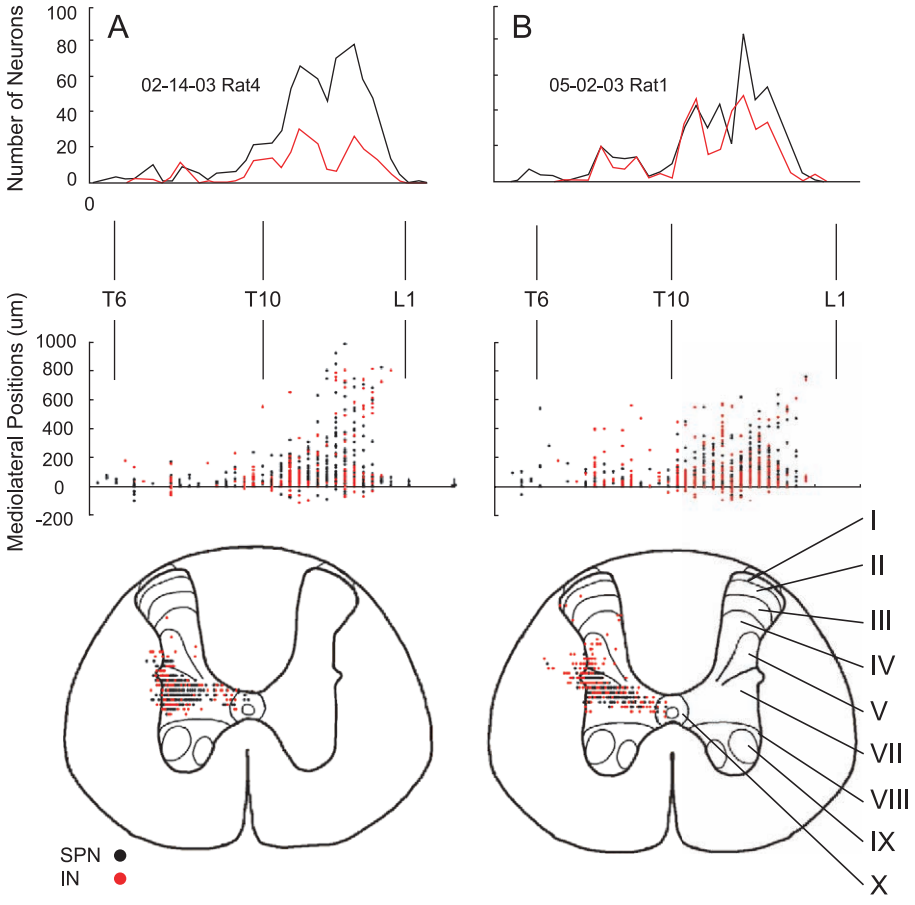


Fig. 2. Panels (A)–(D) are data for each of four rats. Upper panels: longitudinal distribution of infected IN (red lines) and infected SPN (black lines). Numbers of neurons in 240 μ bins are indicated. Positions of segments are indicated at $T_6$, $T_{10}$, and $L_1$. Middle panels: positions of infected IN (red dots) and infected SPN (black dots) as a function of rostrocaudal position (also in 240 μ bins). Zero mediolateral position is the interface between the lateral funiculus and the gray matter of the dorsal horn and intermediate zone. Negative positions are lateral to the gray–white interface. Lower panels: transverse projections for each rat of infected IN (red dots) and SPN (black dots). Where IN and SPN occupy the same position, IN overlie SPN. Laminae are identified on panel (B).

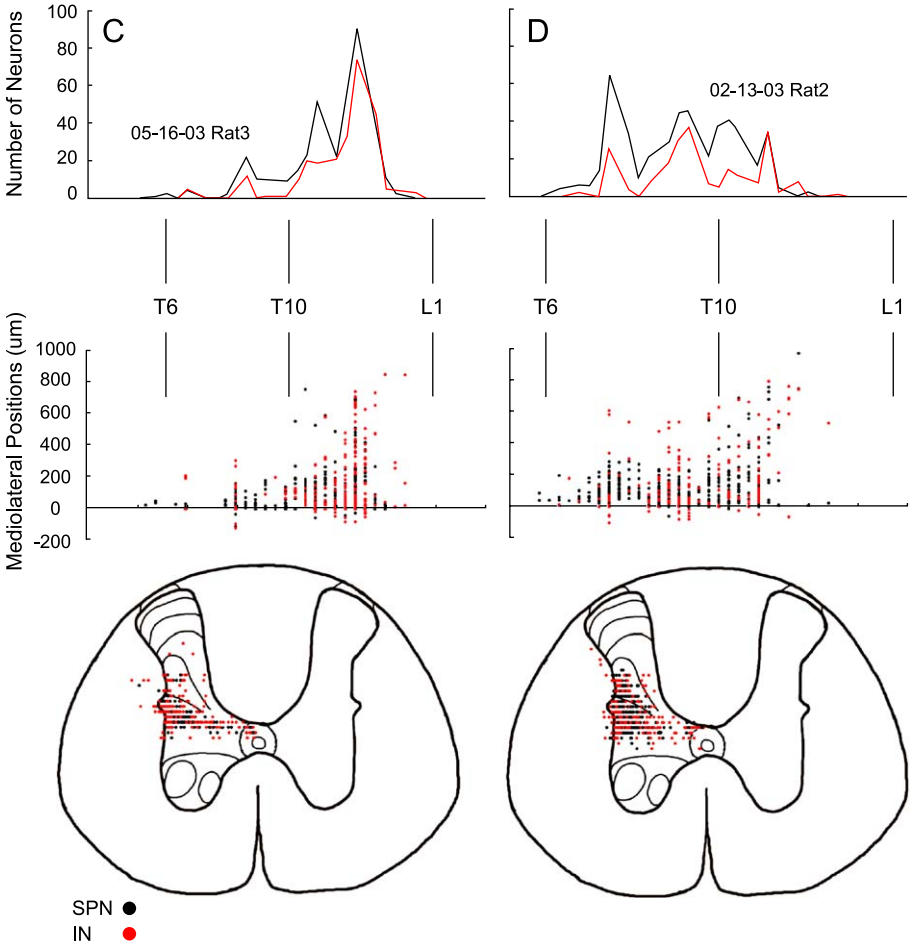


Fig. 2 (*continued*).

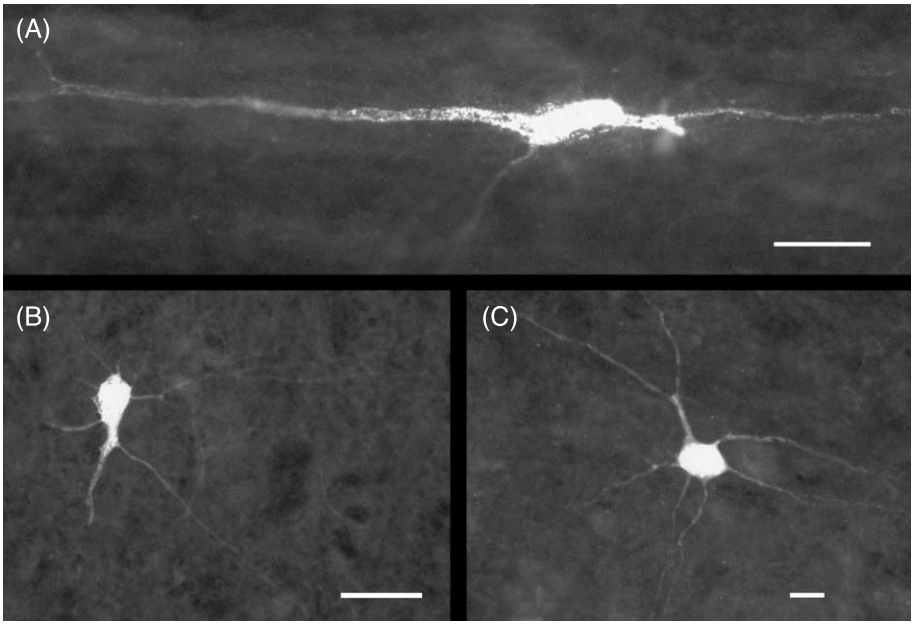


Fig. 3. Morphology of representative PRV-infected IN seen in horizontal sections. In all panels, left is rostral and top is medial. (A) Longitudinally oriented IN, lamina III. (B) Transversely oriented IN, lamina VII. (C) Nonoriented IN, lamina V. All calibration bars=20 μ.

decreased medially and dorsally. The number of infected IN in all lamina was greater in their lateral than in their medial portions. We found an infected IN in lamina I of only one rat. It was located at the ventrolateral border of lamina I, close to the border with lamina II (lower panel, Fig. 2B, lower panel). The sizes, somatic shapes, and dendritic morphologies of infected IN were heterogeneous (Fig. 3).

## 4. Discussion

Although several studies of spinal sympathetic IN have been conducted after tracer injections into a sympathetic ganglion [4] or the adrenal medulla [15], and the presence of sympathetic IN has been noted after injections of pseudorabies virus into the spleen [6] and kidney [5,13,29,30], the present experiments are the first systematic examination of spinal, renal sympathetically related IN. Our use of the term ''sympathetically related'' does not imply that these neurons are employed solely in the regulation of sympathetic activity. Indeed, these neurons also may play roles in the processing of afferent information, in the control of somatic motor functions, or both. Nevertheless, their infection via synapses on SPN indicates, even if their roles are shared, that these IN are capable of affecting sympathetic activity. Similarly, our use of the term ''renal sympathetic preganglionic neurons'' does not imply that these neurons could not share their output with postganglionic neurons that project to organs other than the kidney [5]. By virtue of their synapses on postganglionic neurons that do project to the kidney, however, these SPN are capable of affecting the renal circulation and renal function.

The strong correlation between the longitudinal distributions of infected IN and SPN suggests that the axons of a majority of IN do not traverse the cord longitudinally but, instead, synapse locally on SPN. This observation provides an anatomical substrate that supports the conclusions of physiological studies indicating that many spinal sympathetic reflexes are segmentally organized [7,14,20,29].

We studied the mediolateral distribution of IN in both horizontal and transverse projections. The resulting projections indicated that, in more rostral segments, infected SPN and IN were located almost exclusively in the intermediolateral column and lateral funiculus. Between $T_{11}$ and $T_{13}$, however, infected SPN and IN were also found medially. This distribution suggests that different populations of IN affect SPN at different rostrocaudal levels of the spinal cord.

The transverse distributions of IN (Fig. 2, lower panels) were similar to those reported after injection of the beta unit of cholera toxin or wheat germ agglutinin into the superior cervical ganglion [4], injection of PRV into the spleen [6], or injection of herpes simplex virus type 1 into the adrenal gland [15]. Interneurons were concentrated in lamina VII, the lateral portion of lamina V, and the ventral portion of lamina IV. In addition to locations previously reported, however, we observed a larger number of infected IN in medial lamina IV, and we observed infected IN in laminae I through III. The number of IN was much smaller in the more dorsal laminae. The substantial infection in the lateral portions of lamina V (particularly notable in Fig. 2B and D) is interesting in light of the identification of this region as the ''secondary visceral gray'' by early neuroanatomists [10,33] and by evidence for strong projections to this region by both visceral and somatic primary afferents (see Ref. [19] for review).

Infected interneurons were observed in the same laminae in which we have found neurons with ongoing activities correlated with RSNA [7,8,23,34]. However, fewer infected IN than sympathetically correlated neurons were located in the dorsal and dorsomedial portions of the spinal cord. The wider distribution of sympathetically correlated neurons was expected because, for a three-day survival time, PRV probably did not infect neurons more than one synapse removed from infected SPN, whereas sympathetically correlated neurons could have been many synapses removed from SPN.

The wide range of locations, sizes, shapes, and dendritic morphologies of infected IN supports our observations in juxtacellularly labeled sympathetically correlated neurons [34] and probably manifests the heterogeneity of neural systems capable of affecting sympathetic preganglionic neurons. These systems include axons descending from autonomic regulatory systems in the brain, the axons of primary afferent neurons, axons from neurons located in spinal segments proximal to infected SPN, and axons from neurons located in spinal segments distal to infected SPN (''propriospinal'' axons).

The activities of sympathetically correlated $T_{10}$ IN are affected by both noxious and innocuous stimulation of the dermatomes of distal segments [7,8,18]. Therefore, it is significant that few infected spinal IN were observed beyond the range of infected SPN. How are SPN affected by inputs projecting from distant segments? Neither we nor others have observed evidence for long propriospinal projections directly to SPN. We agree with Cabot et al. [4] that the absence of synapses from long propriospinal neurons directly onto SPN indicates that *intersegmental* effects on SPN must be mediated via propriospinal projections to *intrasegmental* IN, which in turn synapse on SPN.

In summary, spinal IN were infected by renal injections of PRV. The longitudinal distribution of these neurons was strongly correlated to the longitudinal distribution of infected SPN, supporting the ''segmental'' organization of spinal sympathetic processing. The lack of infected IN distal to sites containing infected SPN suggests that multisegmental reflexes are not mediated by long propriospinal axons that synapse directly onto SPN. Instead, these reflexes are more likely mediated by propriospinal axons that synapse on IN located near the affected SPN. Finally, renal sympathetic IN are morphologically heterogeneous, very likely manifesting the variety of systems that affect sympathetic activity.

## Acknowledgements

We thank Dr. Arthur Loewy, both for supplying the pseudorabies virus and antibodies used in this study and for numerous consultations. We thank Ms. Esther Kim, Ms. Julie Schafer, and Ms. Alexis Webb and Mr. Anand Veeravagu for valuable technical assistance. This research was supported by NIH grant HL16315.

## References

[1] C.R. Anderson, S.L. Edwards, Intraperitoneal injections of Fluorogold reliably labels all sympathetic preganglionic neurons in the rat, J. Neurosci. Methods 53 (1994) 137–141.
[2] S.M. Barman, Spinal cord control of the cardiovascular system, in: W.C. Randall (Ed.), Nervous Control of Cardiovascular Function, Oxford Univ. Press, New York, 1984, pp. 321–345.
[3] W.W. Blessing, The Lower Brainstem and Bodily Homeostasis, Oxford Univ. Press, New York, 1997.
[4] J.B. Cabot, V. Alessi, J. Carroll, M. Ligorio, Spinal cord lamina V and lamina VII interneuronal projections to sympathetic preganglionic neurons, J. Comp. Neurol. 347 (1994) 515–530.
[5] G. Cano, Characterization of the CNS control of sympathetic outflow using viral transneuronal tracing. Dissertation submitted to the Graduate Faculty of the Arts and Sciences. University of Pittsburgh, 2002, pp. 156–158.
[6] G. Cano, A.F. Sved, L. Rinaman, B.S. Rabin, J.P. Card, Characterization of the central nervous system innervation of the rat spleen using viral transneuronal tracing, J. Comp. Neurol. 439 (2001) 1–18.
[7] D. Chau, J. Kim, L.P. Schramm, Sympathetically-correlated activities of dorsal horn neurons in spinally transected rats, J. Neurophysiol. 77 (1997) 2966–2974.
[8] D. Chau, D.G. Johns, L.P. Schramm, Ongoing and stimulus-evoked activity of sympathetically correlated neurons in the intermediate zone and dorsal horn of acutely spinalized rats, J. Neurophysiol. 83 (2000) 2699–2707.
[9] J.H. Coote, A. Sato, Supraspinal regulation of spinal reflex discharge into cardiac sympathetic nerves, Brain Res. 142 (1978) 425–437.
[10] E.C. Crosby, T. Humphrey, E.W. Lauer, Correlative Anatomy of the Nervous System, Macmillan, New York, 1962, pp. 67–69.
[11] K. Dembowsky, J. Czachurski, H. Seller, An intracellular study of the synaptic input to sympathetic preganglionic neurones of the third thoracic segment of the cat, J. Auton. Nerv. Syst. 13 (1985) 201–244.
[12] S.A. Deuchars, R.E. Brooke, B. Frater, J. Deuchars, Properties of interneurones in the intermediolateral cell column of the rat spinal cord: role of the potassium channel subunit Kv3.1, Neuroscience 106 (2001) 433–446.
[13] J. Huang, S.I. Chowhdury, M.L. Weiss, Distribution of sympathetic preganglionic neurons innervating the kidney in the rat: PRV transneuronal tracing and serial reconstruction, Auton. Neurosci. 95 (2002) 57–70.
[14] W. Jänig, Spinal cord integration of visceral sensory systems and sympathetic nervous system reflexes, Prog. Brain Res. 67 (1986) 255–277.
[15] S. Joshi, M.A. Levatte, G.A. Dekaban, L.C. Weaver, Identification of spinal interneurons antecedent to adrenal sympathetic preganglionic neurons using trans-synaptic transport of herpes simplex virus type 1, Neuroscience 65 (1995) 893–903.
[16] M.M. Knuepfer, E.W. Akeyson, L.P. Schramm, Spinal projections of renal afferent nerves in the rat, Brain Res. 446 (1998) 17–25.
[17] A.V. Krassioukov, L.C. Weaver, Episodic hypertension due to autonomic dysreflexia in acute and chronic spinal cord injured rats, Am. J. Physiol. 268 (1995) H2077–H2083.
[18] A.V. Krassioukov, D.G. Johns, L.P. Schramm, Sensitivity of sympathetically correlated spinal interneurons, renal sympathetic nerve activity, and arterial pressure to somatic and visceral stimuli after chronic spinal injury, J. Neurotrauma 19 (2002) 1521–1529.
[19] D.C. Kuo, I. Nadelhaft, T. Hisamitsu, W.C. De Groat, Segmental distribution and central projections of renal afferent fibers in the cat studied by transganglionic transport of horseradish peroxidase, J. Comp. Neurol. 216 (1983) 162–174.
[20] W. Laskey, C. Polosa, Characteristics of the sympathetic preganglionic neuron and its synaptic input, Prog. Neurobiol. 32 (1988) 47–84.
[21] Y.-W. Li, Z.-Q. Ding, S.L. Wesselingh, W.W. Blessing, Renal and adrenal sympathetic preganglionic neurons in rabbit spinal cord: tracing with herpes simplex virus, Brain Res. 573 (1992) 147–152.
[22] C.J. Mathias, H.L. Frankel, Autonomic disturbances in spinal cord lesions, in: R. Bannister, C.J. Mathias (Eds.), Autonomic Failure, Oxford Univ. Press, Oxford, 1992, pp. 839–881.
[23] C.O. Miller, D.G. Johns, L.P. Schramm, Spinal interneurons play a minor role in generating ongoing renal sympathetic nerve activity in spinally intact rats, Brain Res. 918 (2001) 101–106.
[24] S.F. Morrison, J. Callaway, T.A. Milner, D.J. Reis, Rostral ventrolateral medulla: a source of the glutamatergic innervation of the sympathetic intermediolateral nucleus, Brain Res. 562 (1991) 126–135.
[25] J.W. Osborn, R.F. Taylor, L.P. Schramm, Chronic cervical spinal cord injury and autonomic hyperreflexia in rats, Am. J. Physiol. 258 (1990) R169–R174.
[26] C.A. Ross, D.A. Ruggiero, T.H. Joh, D.H. Park, D.J. Reis, Rostral ventrolateral medulla: selective projections to the thoracic autonomic cell column from the region containing C1 adrenaline neurons, J. Comp. Neurol. 228 (1984) 168–185.
[27] A. Sato, R.F. Schmidt, Somatosympathetic reflexes: afferent fibers, central pathways, discharge characteristics, Physiol. Rev. 53 (1973) 916–947.
[28] L.P. Schramm, L.R. Poree, Medullo–spinal modulation of sympathetic output and spinal afferent input, J. Cardiovasc. Electrophysiol. 2 (1991) S18–S25.
[29] L.P. Schramm, A.M. Strack, K.B. Platt, A.D. Loewy, Peripheral and central pathways regulating the kidney: a study using pseudorabies virus, Brain Res. 616 (1993) 251–262.
[30] D.J. Sly, L. Colvill, M.J. McKinley, B.J. Oldfield, Identification of neural projection from the forebrain to the kidney, using the virus pseudorabies, J. Auton. Nerv. Syst. 77 (1999) 73–82.
[31] A.M. Strack, A.D. Loewy, Pseudorabies virus: a highly specific transneuronal cell body marker in the sympathetic nervous system, J. Neurosci. 10 (1990) 2139–2147.
[32] A.M. Strack, W.B. Sawyer, J.H. Hughes, K.B. Platt, A.D. Loewy, A general pattern of CNS innervation of the sympathetic outflow demonstrated by transneuronal pseudorabies viral infections, Brain Res. 491 (1989) 156–162.
[33] D. Takahashi, Zur vergleichenden Anatomie des Seitenhorns im Rückenmark der Vertebraten, Arb. Neurol. Inst. Wien. Univ. 20 (1913) 62–83.
[34] X. Tang, N.D. Neckel, L.P. Schramm, The locations and morphologies of sympathetically correlated neurons in the $T_{10}$ spinal segment of the rat, Brain Res. 976 (2003) 185–193.
[35] R.W. Teasell, J.M. Arnold, A. Krassioukov, G.A. Delaney, Cardiovascular consequences of loss of supraspinal control of the sympathetic nervous system after spinal cord injury, Arch. Phys. Med. Rehabil. 4 (2000) 506–516.
[36] L.C. Weaver, C. Polosa, Spinal cord circuits providing control of sympathetic preganglionic neurones, in: D. Jordan (Ed.), The Autonomic Nervous System: Central Nervous Control of Autonomic Function, Harwood Academic, Amsterdam, 1997, pp. 29–61.
[37] M.W. Wessendorf, Fluoro–Gold: composition, and mechanism of uptake, Brain Res. 553 (1991) 135–148.
[38] S.T. Wong, B.A. Atkinson, L.C. Weaver, Confocal microscopic analysis reveals sprouting of primary afferent fibres in rat dorsal horn after spinal cord injury, Neurosci. Lett. 296 (2000) 65–68.